PMU-Aided Voltage Security Assessment for a Wind Power Plant

Preprint

H. Jiang,[1] Y.C. Zhang,[2] J.J. Zhang,[1] and E. Muljadi[2]

[1] *University of Denver*
[2] *National Renewable Energy Laboratory*

To be presented at the 2015 IEEE Power and Energy Society General Meeting
Denver, Colorado
July 26–30, 2015

NREL is a national laboratory of the U.S. Department of Energy
Office of Energy Efficiency & Renewable Energy
Operated by the Alliance for Sustainable Energy, LLC

This report is available at no cost from the National Renewable Energy Laboratory (NREL) at www.nrel.gov/publications.

Conference Paper
NREL/CP-5D00-63846
April 2015

Contract No. DE-AC36-08GO28308

This report is available at no cost from the National Renewable Energy Laboratory (NREL) at www.nrel.gov/publications.

Available electronically at http://www.osti.gov/scitech

Available for a processing fee to U.S. Department of Energy and its contractors, in paper, from:

U.S. Department of Energy
Office of Scientific and Technical Information
P.O. Box 62
Oak Ridge, TN 37831-0062
phone: 865.576.8401
fax: 865.576.5728
email: mailto:reports@adonis.osti.gov

Available for sale to the public, in paper, from:

U.S. Department of Commerce
National Technical Information Service
5285 Port Royal Road
Springfield, VA 22161
phone: 800.553.6847
fax: 703.605.6900
email: orders@ntis.fedworld.gov
online ordering: http://www.ntis.gov/help/ordermethods.aspx

Cover Photos: (left to right) photo by Pat Corkery, NREL 16416, photo from SunEdison, NREL 17423, photo by Pat Corkery, NREL 16560, photo by Dennis Schroeder, NREL 17613, photo by Dean Armstrong, NREL 17436, photo by Pat Corkery, NREL 17721.

NREL prints on paper that contains recycled content.

PMU-Aided Voltage Security Assessment for a Wind Power Plant

Huaiguang Jiang[1], *Student Member*, IEEE, Yingchen Zhang[2], *Member,* IEEE,
Jun Jason Zhang[1], *Senior Member,* IEEE, Eduard Muljadi[2], *Fellow,* IEEE
[1]Department of Electrical and Computer Engineering, University of Denver, Denver, CO 80210
[2]National Renewable Energy Laboratory, Golden, CO 80401

***Abstract*—Because wind power penetration levels in electric power systems are continuously increasing, voltage stability is a critical issue for maintaining power system security and operation. The traditional methods to analyze voltage stability can be classified into two categories: dynamic and steady-state. Dynamic analysis relies on time-domain simulations of faults at different locations; however, this method needs to exhaust faults at all locations to find the security region for voltage at a single bus. With the widely located phasor measurement units (PMUs), the Thevenin equivalent matrix can be calculated by the voltage and current information collected by the PMUs. This paper proposes a method based on a Thevenin equivalent matrix to identify system locations that will have the greatest impact on the voltage at the wind power plant's point of interconnection. The number of dynamic voltage stability analysis runs is greatly reduced by using the proposed method. The numerical results demonstrate the feasibility, effectiveness, and robustness of the proposed approach for voltage security assessment for a wind power plant.**

***Index Terms*—Power system, phasor measurement unit, fault disturbance recorder, wind power plant, voltage security**

I. Introduction

With the increasing technology of wind turbines, the penetration level of wind power is rising and wind power has become competitive with other types of generation. Because of the low penetration levels of wind power during the early decades, the loss of a wind power plant was not considered a critical threat to power system security. During these decades, when a fault caused the voltage deviation at the interconnection bus of a wind power plant, the wind power plant was disconnected and reconnected when the fault was cleared and the voltage returned to normal [1]–[3]. In the modern power systems, because the size of wind power plant have increased (up to 1,000 MW), wind power is an indispensable resource in generation, and the simple disconnection-reconnection approach cannot be adopted for voltage deviation scenarios. Therefore, it is imperative to develop an effective and efficient voltage assessment approach to enhance voltage security for wind power plants.

Voltage stability assessment methods in power systems can be classified into two categories: dynamic simulation and steady-state. A dynamic simulation is a method in which a high-accuracy dynamic test bench is built to determine the fault impact. To generate an accurate analysis of voltage stability, the dynamic test bench includes excitation systems, capacitors, high-order generator models, relay protections, and so on. In [4], the dynamic simulation provides a more accurate result than that of the V-Q power flow simulation. In [5], dynamic wind turbine models are built to study the voltage stability of the power system with a large amount of wind power. Although the dynamic approach is accurate, this method relies on time-domain simulations of faults at different locations. Ref. [6] illustrates that steady-state analysis provides another effective way to analyze voltage stability. In [7], a steady-state method is used to assess voltage security by using decision tree. In [8], by using times-series power flow, a steady-state method is used to analyze voltage stability of power system with high penetrations of wind. By using artificial intelligence in [9], a steady-state method is used to analyze voltage stability of power system. Assuming the involved dynamics are very slow, a steady-state method is designed for the voltage collapse analysis [10]–[12].

Recently, synchrophasor measurement devices, such as phasor measurement units (PMUs), have been used to measure power system monitoring. Widely distributed synchrophasor sensors can record the multimodal signals in high speed for power system situational awareness, such as voltage and current phasors, frequency and rate of change of frequency [13]–[15]. Based on the multimodal PMU monitoring system, this paper proposes a novel voltage security assessment for a wind power plant. First, in the power system, a PMU can collect information about power flow, voltage, and current phasors in real time. Second, by using these real-time measurements, the Thevenin equivalent impedance between every bus can be derived. Third, this matrix indicates the impact of the change in current injection at one bus on other buses during balanced fault conditions. By examining this matrix, the location of a fault can be derived when it occurs and has a large impact on a wind power plant's point of interconnection [1]. The proposed method is different from the traditional methods, because it provides an effective and robust way to assess the voltage security of a wind power plant, especially in a bulk power system that has unknown parameters.

The paper is organized as follows. Section II describes the voltage security problem formulation and the flowchart of the proposed approach. Section III calculates the PMUs-aided Thevenin equivalent matrix. Section IV presents the steady-state voltage stability assessment for different scenarios. Section V presents numerical results of the proposed approach.

II. Voltage Security Assessment Problem Formulation

As discussed in Section I, a PMU-aided voltage security assessment approach is proposed in this paper for power systems that have a wind power plant. The objective of voltage security assessment is to identify system locations that will have the greatest impact on the voltage at the wind power plant's point of interconnection. Considering that a three-phase

This work was supported by the U.S. Department of Energy under Contract No. DE-AC36-08-GO28308 with the National Renewable Energy Laboratory.

symmetrical fault on a bus causes the highest fault current, it is necessary to study it to better protect the wind power plant in the system. Thus, this paper studies the three-phase symmetrical fault to illustrate the proposed approach. It is assumed that the PMUs are located on all the buses in the power system.

The voltage $\mathbf{V} = [V_1, V_2, V_3, \cdots, V_n]$ measured by PMUs at each bus, and $n = 1, 2, 3, \cdots$ is the bus number. $\mathbf{V}^0 = [V_1^0, V_2^0, V_3^0, \cdots, V_n^0]$ indicates the bus voltage pre-fault condition. $\Delta\mathbf{V} = [\Delta V_1, \Delta V_2, \Delta V_3, \cdots, \Delta V_n]$ indicates the calculated voltage deviation during the fault condition. The current $\mathbf{I} = [I_1, I_2, I_3, \cdots, I_n]$ measured by PMUs at each bus. The element $[I_{ij}^{Tr}]$ in the current matrix $\mathbf{I}^{Tr}$ indicates the current from bus i to bus j, and i, j are the bus numbers. $\mathbf{I}^{SC} = [I_1^{SC}, I_2^{SC}, I_3^{SC}, \cdots, I_n^{SC}]$ is the short-circuit current for a fault at bus n, n is defined as above. The element $[Z_{i,j}]$ in impedance matrix $\mathbf{Z}$ indicates the Thevenin equivalent impedance between bus i and bus j. The element $[Y_{i,j}]$ in admittance matrix $\mathbf{Y}$ indicates the admittance between bus i and bus j. $\mathbf{B}$ is the critical bus number set, which has the greatest voltage deviation at the wind power plant's point of interconnection.

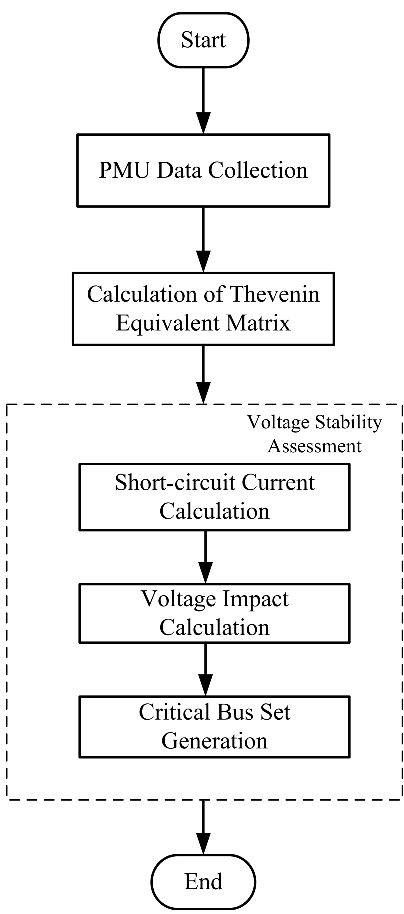

Fig. 1. Flowchart of the voltage stability assessment approach.

The flowchart shown in Fig. 1 illustrates the architecture of the proposed approach. At the first step, the voltage and current information $\mathbf{V}$, $\mathbf{V}^0$, $\mathbf{I}$ and $\mathbf{I}^{Tr}$ are collected by the PMUs equipped on every bus. Second, with the voltage and current information, the Thevenin equivalent matrix $\mathbf{Z}$ can be calculated. Third, with the Thevenin equivalent matrix $\mathbf{Z}$ and the bus voltage pre-fault condition $\mathbf{V}^0$, the short-circuit current $\mathbf{I}^{SC}$ and the voltage deviation $\Delta\mathbf{V}$ can be calculated. The critical bus set $\mathbf{B}$ is generated, which has the greatest impact on the voltage stability at the wind power plant's point of interconnection. Finally, in the numerical simulation results, the dynamic simulation is used to verify the proposed voltage security assessment approach.

III. PMU-aided Thevenin Equivalent Matrix

Traditionally, the Thevenin equivalent matrix can be calculated using the measurement of open-circuit voltage and short-circuit current. In this paper, because a PMU is located at every bus in the power system, a direct calculation method is used to generate the Thevenin equivalent matrix.

A. Thevenin Impedance at Bus

Because the voltage $\mathbf{V}$ and current $\mathbf{I}$ indicates the voltage and current information of every bus, respectively, the Thevenin impedance can be calculated as follows:

$$Z_i = V_i / I_i, \tag{1}$$

where $i = 1, 2, 3, \cdots, n$; i is the bus number.

Similarly, the Thevenin impedance between bus i and bus j can be calculated using the voltage and current information collected by the PMUs. The voltage between bus i and bus j can be calculated as

$$V_{ij} = V_i - V_j, \tag{2}$$

where $i, j = 1, 2, 3, \cdots, n$; i, j are the bus numbers. Then, with the current I_{ij}^{Tr} measured by the PMU, which indicates the current between bus i and bus j. The Thevenin impedance between bus i and bus j can be calculated as

$$Z_{ij} = V_{ij} / I_{ij}, \tag{3}$$

This method provides an effective and robust way to calculate the Thevenin equivalent matrix without knowing the impedance or admittance information of the power system.

B. A Demonstration on an IEEE 14-Bus System

An illustration of the IEEE 14-bus system is in Fig. 2. By using the collected voltage and current information $\mathbf{V}$, $\mathbf{I}$ and $\mathbf{I}^{Tr}$, the Thevenin equivalent matrix can be calculated in Table I. Considering the nature hazards, such as typhoon and earthquake, the parameters and the topology of power systems will change. For this IEEE 14-bus power system, it is assumed that the transmission line between bus 13 and 14, and bus 11 and 10 are outaged. The Thevenin equivalent matrix can be calculated as shown in Table II.

TABLE I
THE THEVENIN EQUIVALENT MATRIX OF AN IEEE 14-BUS SYSTEM

Bus No.	*1*	*2*	*3*	*4*	*5*	*6*	*7*
1	-0.2616 - 2.2206i	-0.2728 - 2.2587i	-0.2781 - 2.2847i	-0.2837 - 2.2940i	-0.2783 - 2.2812i	-0.2886 - 2.4460i	-0.2969 - 2.4127i
2	-0.2728 - 2.2587i	-0.2683 - 2.2472i	-0.2752 - 2.2785i	-0.2830 - 2.2925i	-0.2788 - 2.2830i	-0.2890 - 2.4467i	-0.2963 - 2.4118i
3	-0.2781 - 2.2847i	-0.2752 - 2.2785i	-0.2494 - 2.1984i	-0.2812 - 2.2883i	-0.2794 - 2.2884i	-0.2894 - 2.4490i	-0.2946 - 2.4093i
4	-0.2837 - 2.2940i	-0.2830 - 2.2925i	-0.2812 - 2.2883i	-0.2768 - 2.2715i	-0.2783 - 2.2799i	-0.2876 - 2.4368i	-0.2903 - 2.3933i
5	-0.2783 - 2.2812i	-0.2788 - 2.2830i	-0.2794 - 2.2884i	-0.2783 - 2.2799i	-0.2694 - 2.2545i	-0.2797 - 2.4220i	-0.2910 - 2.3953i
6	-0.2886 - 2.4460i	-0.2890 - 2.4467i	-0.2894 - 2.4490i	-0.2876 - 2.4368i	-0.2797 - 2.4220i	-0.2766 - 2.4279i	-0.3086 - 2.5176i
7	-0.2969 - 2.4127i	-0.2963 - 2.4118i	-0.2946 - 2.4093i	-0.2903 - 2.3933i	-0.2910 - 2.3953i	-0.3086 - 2.5176i	-0.3000 - 2.3824i
8	-0.2969 - 2.4127i	-0.2963 - 2.4118i	-0.2946 - 2.4093i	-0.2903 - 2.3933i	-0.2910 - 2.3953i	-0.3086 - 2.5176i	-0.3000 - 2.3824i
9	-0.3004 - 2.4474i	-0.2998 - 2.4468i	-0.2982 - 2.4452i	-0.2940 - 2.4299i	-0.2943 - 2.4284i	-0.3162 - 2.5307i	-0.3017 - 2.4577i
10	-0.2979 - 2.4462i	-0.2975 - 2.4458i	-0.2961 - 2.4449i	-0.2923 - 2.4302i	-0.2914 - 2.4264i	-0.3098 - 2.5116i	-0.3018 - 2.4673i
11	-0.2920 - 2.4437i	-0.2920 - 2.4439i	-0.2914 - 2.4446i	-0.2886 - 2.4311i	-0.2844 - 2.4219i	-0.2932 - 2.4682i	-0.3032 - 2.4896i
12	-0.2846 - 2.4482i	-0.2849 - 2.4488i	-0.2852 - 2.4508i	-0.2833 - 2.4384i	-0.2758 - 2.4246i	-0.2734 - 2.4376i	-0.3038 - 2.5154i
13	-0.2858 - 2.4460i	-0.2860 - 2.4465i	-0.2861 - 2.4483i	-0.2840 - 2.4357i	-0.2774 - 2.4227i	-0.2785 - 2.4424i	-0.3025 - 2.5089i
14	-0.2941 - 2.4467i	-0.2938 - 2.4466i	-0.2929 - 2.4465i	-0.2896 - 2.4324i	-0.2870 - 2.4259i	-0.3003 - 2.4921i	-0.3018 - 2.4800i

Bus No.	*8*	*9*	*10*	*11*	*12*	*13*	*14*
1	-0.2616 - 2.2206i	-0.2728 - 2.2587i	-0.2781 - 2.2847i	-0.2837 - 2.2940i	-0.2783 - 2.2812i	-0.2886 - 2.4460i	-0.2969 - 2.4127i
2	-0.2728 - 2.2587i	-0.2683 - 2.2472i	-0.2752 - 2.2785i	-0.2830 - 2.2925i	-0.2788 - 2.2830i	-0.2890 - 2.4467i	-0.2963 - 2.4118i
3	-0.2781 - 2.2847i	-0.2752 - 2.2785i	-0.2494 - 2.1984i	-0.2812 - 2.2883i	-0.2794 - 2.2884i	-0.2894 - 2.4490i	-0.2946 - 2.4093i
4	-0.2837 - 2.2940i	-0.2830 - 2.2925i	-0.2812 - 2.2883i	-0.2768 - 2.2715i	-0.2783 - 2.2799i	-0.2876 - 2.4368i	-0.2903 - 2.3933i
5	-0.2783 - 2.2812i	-0.2788 - 2.2830i	-0.2794 - 2.2884i	-0.2783 - 2.2799i	-0.2694 - 2.2545i	-0.2797 - 2.4220i	-0.2910 - 2.3953i
6	-0.2886 - 2.4460i	-0.2890 - 2.4467i	-0.2894 - 2.4490i	-0.2876 - 2.4368i	-0.2797 - 2.4220i	-0.2766 - 2.4279i	-0.3086 - 2.5176i
7	-0.2969 - 2.4127i	-0.2963 - 2.4118i	-0.2946 - 2.4093i	-0.2903 - 2.3933i	-0.2910 - 2.3953i	-0.3086 - 2.5176i	-0.3000 - 2.3824i
8	-0.2969 - 2.4127i	-0.2963 - 2.4118i	-0.2946 - 2.4093i	-0.2903 - 2.3933i	-0.2910 - 2.3953i	-0.3086 - 2.5176i	-0.3000 - 2.3824i
9	-0.3004 - 2.4474i	-0.2998 - 2.4468i	-0.2982 - 2.4452i	-0.2940 - 2.4299i	-0.2943 - 2.4284i	-0.3162 - 2.5307i	-0.3017 - 2.4577i
10	-0.2979 - 2.4462i	-0.2975 - 2.4458i	-0.2961 - 2.4449i	-0.2923 - 2.4302i	-0.2914 - 2.4264i	-0.3098 - 2.5116i	-0.3018 - 2.4673i
11	-0.2920 - 2.4437i	-0.2920 - 2.4439i	-0.2914 - 2.4446i	-0.2886 - 2.4311i	-0.2844 - 2.4219i	-0.2932 - 2.4682i	-0.3032 - 2.4896i
12	-0.2846 - 2.4482i	-0.2849 - 2.4488i	-0.2852 - 2.4508i	-0.2833 - 2.4384i	-0.2758 - 2.4246i	-0.2734 - 2.4376i	-0.3038 - 2.5154i
13	-0.2858 - 2.4460i	-0.2860 - 2.4465i	-0.2861 - 2.4483i	-0.2840 - 2.4357i	-0.2774 - 2.4227i	-0.2785 - 2.4424i	-0.3025 - 2.5089i
14	-0.2941 - 2.4467i	-0.2938 - 2.4466i	-0.2929 - 2.4465i	-0.2896 - 2.4324i	-0.2870 - 2.4259i	-0.3003 - 2.4921i	-0.3018 - 2.4800i

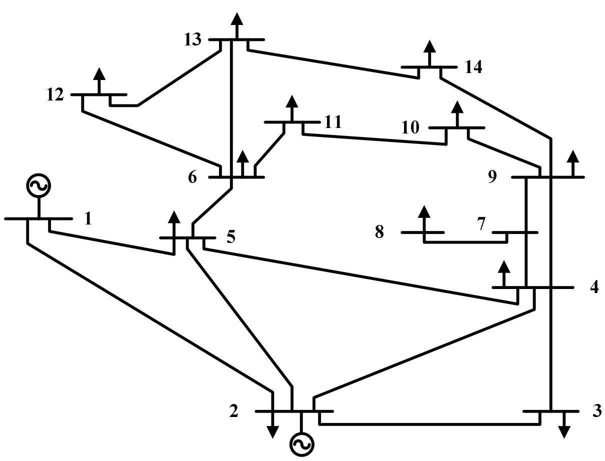

Fig. 2. IEEE 14-bus system.

IV. STEADY-STATE VOLTAGE STABILITY ASSESSMENT

A. Voltage Impact Calculation

Traditionally, the element $[Y_{i,j}]$ in admittance matrix **Y** indicates the admittance between bus i and bus j. And the impedance matrix can be calculated by using the inverse of the admittance matrix **Y** [1]. In this paper, the Thevenin equivalent matrix is used to generate the information on the impact that changes in current injection at one bus have on the others. Because there is a wind power plant in the power system, this approach can be used to generate for the critical bus set **B**, which has the greatest impact on the voltage stability at the wind power plant's point of interconnection. The Thevenin equivalent matrix can be expressed as

$$Z = \begin{bmatrix} Z_{11} & \cdots & Z_{1i} & \cdots & Z_{1n} \\ \cdots & \cdots & \cdots & \cdots & \cdots \\ Z_{i1} & \cdots & Z_{ii} & \cdots & Z_{in} \\ \cdots & \cdots & \cdots & \cdots & \cdots \\ Z_{n1} & \cdots & Z_{ni} & \cdots & Z_{nn} \end{bmatrix},$$

It is assumed that the three-phase symmetrical fault occurs at bus i and the wind power plant is connected at bus j. The short-circuit current at bus i can be calculated as

$$I_i^{SC} = V_i^0 / Z_{ii}, \qquad (4)$$

where:
V_i^0 is the bus voltage pre-fault condition measured by PMUs
Z_{ii} is the Thevenin equivalent impedance of bus i
I_i^{SC} is the short-circuit current at bus i. Then the impact of the fault on bus j can be calculated as

$$\Delta V_j = I_i^{SC} Z_{ij}, \qquad (5)$$

where:
ΔV_j is the fault impact on bus j
Z_{ij} is the Thevenin equivalent impedance between bus i and j

Therefore, all the buses $i = 1, 2, 3, \cdots, n$ can be calculated, and the critical bus set **B** can be determined according to the voltage impacts.

B. A Demonstration on an IEEE 14-bus System

As illustrated before, it is assumed that a wind power plant is located as Bus 10. The voltage impact from large to small is $\{9, 7, 6, 11, 13, 4, 14, 5, 2, 12, 1, 3, 8\}$. Because the

TABLE II
THE THEVENIN EQUIVALENT MATRIX OF AN IEEE 14-BUS SYSTEM FOR TRANSMISSION LINE OUTAGE

Bus No.	*1*	*2*	*3*	*4*	*5*	*6*	*7*
1	-0.1806 - 2.1196i	-0.1919 - 2.1577i	-0.1975 - 2.1836i	-0.2039 - 2.1935i	-0.1978 - 2.1809i	-0.2005 - 2.3412i	-0.2181 - 2.3114i
2	-0.1919 - 2.1577i	-0.1875 - 2.1461i	-0.1946 - 2.1774i	-0.2032 - 2.1918i	-0.1985 - 2.1828i	-0.2012 - 2.3432i	-0.2174 - 2.3097i
3	-0.1975 - 2.1836i	-0.1946 - 2.1774i	-0.1691 - 2.0971i	-0.2016 - 2.1873i	-0.1995 - 2.1883i	-0.2022 - 2.3492i	-0.2157 - 2.3049i
4	-0.2039 - 2.1935i	-0.2032 - 2.1918i	-0.2016 - 2.1873i	-0.1978 - 2.1708i	-0.1992 - 2.1805i	-0.2020 - 2.3408i	-0.2116 - 2.2876i
5	-0.1978 - 2.1809i	-0.1985 - 2.1828i	-0.1995 - 2.1883i	-0.1992 - 2.1805i	-0.1894 - 2.1546i	-0.1916 - 2.3130i	-0.2132 - 2.2978i
6	-0.2005 - 2.3412i	-0.2012 - 2.3432i	-0.2022 - 2.3492i	-0.2020 - 2.3408i	-0.1916 - 2.3130i	-0.1944 - 2.2310i	-0.2163 - 2.4667i
7	-0.2181 - 2.3114i	-0.2174 - 2.3097i	-0.2157 - 2.3049i	-0.2116 - 2.2876i	-0.2132 - 2.2978i	-0.2163 - 2.4667i	-0.2262 - 2.2478i
8	-0.2181 - 2.3114i	-0.2174 - 2.3097i	-0.2157 - 2.3049i	-0.2116 - 2.2876i	-0.2132 - 2.2978i	-0.2163 - 2.4667i	-0.2262 - 2.2478i
9	-0.2231 - 2.3469i	-0.2224 - 2.3452i	-0.2207 - 2.3403i	-0.2165 - 2.3227i	-0.2181 - 2.3331i	-0.2215 - 2.5046i	-0.2314 - 2.3091i
10	-0.2231 - 2.3469i	-0.2224 - 2.3452i	-0.2207 - 2.3403i	-0.2165 - 2.3227i	-0.2181 - 2.3331i	-0.2215 - 2.5046i	-0.2314 - 2.3091i
11	-0.2005 - 2.3412i	-0.2012 - 2.3432i	-0.2022 - 2.3492i	-0.2020 - 2.3408i	-0.1916 - 2.3130i	-0.1944 - 2.2310i	-0.2163 - 2.4667i
12	-0.1972 - 2.3436i	-0.1979 - 2.3457i	-0.1989 - 2.3516i	-0.1987 - 2.3433i	-0.1884 - 2.3154i	-0.1912 - 2.2333i	-0.2129 - 2.4693i
13	-0.1992 - 2.3417i	-0.1999 - 2.3437i	-0.2010 - 2.3497i	-0.2007 - 2.3413i	-0.1904 - 2.3135i	-0.1932 - 2.2315i	-0.2150 - 2.4673i
14	-0.2231 - 2.3469i	-0.2224 - 2.3452i	-0.2207 - 2.3403i	-0.2165 - 2.3227i	-0.2181 - 2.3331i	-0.2215 - 2.5046i	-0.2314 - 2.3091i

Bus No.	*8*	*9*	*10*	*11*	*12*	*13*	*14*
1	-0.2181 - 2.3114i	-0.2231 - 2.3469i	-0.2231 - 2.3469i	-0.2005 - 2.3412i	-0.1972 - 2.3436i	-0.1992 - 2.3417i	-0.2231 - 2.3469i
2	-0.2174 - 2.3097i	-0.2224 - 2.3452i	-0.2224 - 2.3452i	-0.2012 - 2.3432i	-0.1979 - 2.3457i	-0.1999 - 2.3437i	-0.2224 - 2.3452i
3	-0.2157 - 2.3049i	-0.2207 - 2.3403i	-0.2207 - 2.3403i	-0.2022 - 2.3492i	-0.1989 - 2.3516i	-0.2010 - 2.3497i	-0.2207 - 2.3403i
4	-0.2116 - 2.2876i	-0.2165 - 2.3227i	-0.2165 - 2.3227i	-0.2020 - 2.3408i	-0.1987 - 2.3433i	-0.2007 - 2.3413i	-0.2165 - 2.3227i
5	-0.2132 - 2.2978i	-0.2181 - 2.3331i	-0.2181 - 2.3331i	-0.1916 - 2.3130i	-0.1884 - 2.3154i	-0.1904 - 2.3135i	-0.2181 - 2.3331i
6	-0.2163 - 2.4667i	-0.2215 - 2.5046i	-0.2215 - 2.5046i	-0.1944 - 2.2310i	-0.1912 - 2.2333i	-0.1932 - 2.2315i	-0.2215 - 2.5046i
7	-0.2262 - 2.2478i	-0.2314 - 2.3091i	-0.2314 - 2.3091i	-0.2163 - 2.4667i	-0.2129 - 2.4693i	-0.2150 - 2.4673i	-0.2314 - 2.3091i
8	-0.2262 - 2.0717i	-0.2314 - 2.3091i	-0.2314 - 2.3091i	-0.2163 - 2.4667i	-0.2129 - 2.4693i	-0.2150 - 2.4673i	-0.2314 - 2.3091i
9	-0.2314 - 2.3091i	-0.2365 - 2.2739i	-0.2365 - 2.2739i	-0.2215 - 2.5046i	-0.2179 - 2.5072i	-0.2201 - 2.5052i	-0.2365 - 2.2739i
10	-0.2314 - 2.3091i	-0.2365 - 2.2739i	-0.2048 - 2.1894i	-0.2215 - 2.5046i	-0.2179 - 2.5072i	-0.2201 - 2.5052i	-0.2365 - 2.2739i
11	-0.2163 - 2.4667i	-0.2215 - 2.5046i	-0.2215 - 2.5046i	-0.0991 - 2.0322i	-0.1912 - 2.2333i	-0.1932 - 2.2315i	-0.2215 - 2.5046i
12	-0.2129 - 2.4693i	-0.2179 - 2.5072i	-0.2179 - 2.5072i	-0.1912 - 2.2333i	-0.0971 - 2.0878i	-0.1726 - 2.1785i	-0.2179 - 2.5072i
13	-0.2150 - 2.4673i	-0.2201 - 2.5052i	-0.2201 - 2.5052i	-0.1932 - 2.2315i	-0.1726 - 2.1785i	-0.1354 - 2.1300i	-0.2201 - 2.5052i
14	-0.2314 - 2.3091i	-0.2365 - 2.2739i	-0.2365 - 2.2739i	-0.2215 - 2.5046i	-0.2179 - 2.5072i	-0.2201 - 2.5052i	-0.1097 - 2.0033i

IEEE 14-bus system is relatively small, if there is a three-phase symmetrical fault occurs at Bus 10, the whole power system will be impacted heavily. So considering the greatest voltage impact, the first 30% voltage deviation impact buses are chosen, and the critical bus set is determined as $\{9, 7, 6, 11\}$.

Considering the nature hazards, the transmission lines between Bus 13 and 14, and Bus 11 and 10 are outage. As above, the voltage impact from large to small is $\{9, 7, 4, 5, 2, 1, 8, 3, 6, 14, 13, 12, 11\}$. The critical bus set can be determined as $\{9, 7, 4, 5\}$.

V. NUMERICAL SIMULATION AND RESULTS

In the numerical simulation, the IEEE 14-bus system and IEEE 39-bus system are built in the simulation tool PowerWorld. It is assumed that a PMU is equipped at every bus, which provides real-time data acquisition. And the sample rate of the PMUs is 1 kHz.

A. Numerical Simulation for an IEEE 14-Bus System

As discussed above, the steady-state voltage stability assessment approach gives two critical bus sets, which indicate the greatest impact on the voltage at the interconnection point of a wind power plant.

To verify the results, the three-phase symmetrical fault is simulated in PowerWorld. For the normal condition scenario, the critical bus set is $\{9, 7, 11, 6\}$. For the transmission outage scenario, the critical bus set is $\{9, 7, 4, 5\}$. The results of the dynamic simulations consistently demonstrate the effectiveness and robustness of the proposed approach.

B. Numerical Simulation for an IEEE 39-Bus System

As shown in Fig. 3, the IEEE 39-bus system contains 10 generators, 46 transmission lines, 12 transformers, and 19 loads. It is assumed that a wind power plant is located at Bus 17. Because the IEEE 39-bus system is larger than the IEEE 14-bus system, the three-phase symmetrical fault will not heavily impact the whole power system.

In this condition, the criterion of voltage drop of the wind power plant's interconnection as the bus is that the voltage drop is below 80% of normal. Considering the nature hazards, the transmission lines between Bus 16 and 17, and Bus 25 and 26 are outaged. The numerical simulation of the proposed approach is illustrated in Table III. To verify the results, the three-phase symmetrical fault is simulated in PowerWorld. The simulation results are illustrated in Table IV.

Comparing the result of the proposed approach to the dynamic simulation, the critical bus sets of the proposed approach contain the critical bus sets of the dynamic simulation in the normal scenario and transmission line outage scenario, respectively. Because the proposed approach does not contain all the elements of the relay protection, it is a conservative, but as additional basic dynamic information about the power system is available, the proposed approach will become more accurate.

VI. CONCLUSION

This paper proposed a steady-state PMU-aided voltage security assessment for a wind power plant. The Thevenin matrix is calculated with the data collected by the PMUs. With this matrix, the fault impact of the power system can be calculated for every bus. Then the critical bus set can be generated for the bus at the wind power plant's interconnection. Compared

TABLE III

VOLTAGE STABILITY ASSESSMENT WITH THE PROPOSED APPROACH

Scenario Type	Voltage Impact Size	Critical Bus
Normal Condition	18 16 27 3 15 24 4 14 2 5 6 25 13 26 30 21 22 23 19 10 11 39 12 37 7 8 32 35 31 28 29 20 33 36 1 9 38 34	18 16 27 3 15 24 4 14 2 5 6 25 13 26 30 21 22 23 19 10
Transmission Line Outage	18 27 26 3 28 4 2 5 6 29 8 38 30 7 10 25 1 37 39 15 12 14 9 11 13 32 31 16 24 21 22 23 19 34 36 35 20 33	18 27 26 3 28 4 2 5 6 29 8 38 30 7 10 25 1 37

TABLE IV

VOLTAGE STABILITY ASSESSMENT WITH THE DYNAMIC SIMULATION

Scenario Type	Voltage Impact Size	Critical Bus
Normal Condition	18 27 16 24 15 3 21 26 22 23 2 19 14 4 25 30 20 33 35 13 12 28 10 11 5 6 37 7 8 34 36 29 31 32 1 9 38 39	18 27 16 24 15 3 21 26 22 23 2 19 14 4 25 30
Transmission Line Outage	27 18 26 28 3 29 2 38 30 25 37 4 1 8 31 5 7 39 6 12 14 9 11 13 10 32 15 16 24 20 21 33 34 23 19 22 35 36	27 18 26 28 3 29 2 38 30 25 37 4 1

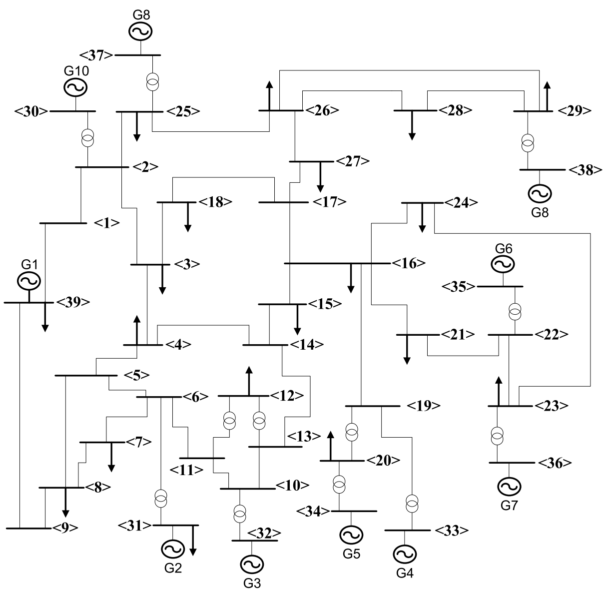

Fig. 3. IEEE 39-bus system.

to the dynamic simulation, the proposed approach is more effective and requires fewer computations. With the present result, the proposed approach is conservative. But combined with the basic dynamic information, the proposed approach can be used to assess the voltage security for a wind power plant in power systems. The nature hazards, such as typhoon and earthquake, will change the parameters of power systems. If the parameters of power system are changed, the proposed approach provides a robust and feasible way to generate the critical bus set. The proposed approach enhances the voltage security and system resilience of power systems.

REFERENCES

[1] E. Muljadi, C. Butterfield, J. Conto, and K. Donohoo, "Ride-through capability predictions for wind power plants in the ercot network," in *Power Engineering Society General Meeting, 2005. IEEE*. IEEE, 2005, pp. 72–79.

[2] H. Jiang, J. J. Zhang, and D. W. Gao, "Fault localization in smart grid using wavelet analysis and unsupervised learning," *2012 Conference Record of the Forty Sixth Asilomar Conference on Signals, Systems and Computers (ASILOMAR)*, pp. 386–390, 2012.

[3] H. Jiang, J. J. Zhang, W. Gao, and Z. Wu, "Fault detection, identification, and location in smart grid based on data-driven computational methods," *IEEE Transactions on Smart Grid*, vol. 5, pp. 2947 – 2956, 2014.

[4] B. H. Chowdhury and C. W. Taylor, "Voltage stability analysis: VQ power flow simulation versus dynamic simulation," *IEEE Transactions on Power Systems*, vol. 15, no. 4, pp. 1354–1359, 2000.

[5] Z. Bi and C. Gao, "Power system dynamic voltage stability analysis considering wind power," in *2014 IEEE 12th International Conference on Dependable, Autonomic and Secure Computing (DASC)*. IEEE, 2014, pp. 129–132.

[6] G. Morison, B. Gao, and P. Kundur, "Voltage stability analysis using static and dynamic approaches," *IEEE Transactions on Power Systems*, vol. 8, no. 3, pp. 1159–1171, 1993.

[7] N. Hatziargyriou, G. Contaxis, and N. Sideris, "A decision tree method for on-line steady state security assessment," *IEEE Transactions on Power Systems*, vol. 9, no. 2, pp. 1052–1061, 1994.

[8] E. Vittal, M. O'Malley, and A. Keane, "A steady-state voltage stability analysis of power systems with high penetrations of wind," *IEEE Transactions on Power Systems*, vol. 25, no. 1, pp. 433–442, 2010.

[9] B. Jeyasurya, "Artificial neural networks for power system steady-state voltage instability evaluation," *Electric power systems research*, vol. 29, no. 2, pp. 85–90, 1994.

[10] A. Berizzi, P. Marannino, M. Merlo, M. Pozzi, and F. Zanellini, "Steady-state and dynamic approaches for the evaluation of loadability margins in the presence of secondary voltage regulation," *IEEE Transactions on Power Systems*, vol. 19, no. 2, pp. 1048–1057, 2004.

[11] A. Berizzi, P. Bresesti, P. Marannino, G. Granelli, and M. Montagna, "System-area operating margin assessment and security enhancement against voltage collapse," *IEEE Transactions on Power Systems*, vol. 11, no. 3, pp. 1451–1462, 1996.

[12] A. Berizzi, P. Finazzi, D. Dosi, P. Marannino, and S. Corsi, "First and second order methods for voltage collapse assessment and security enhancement," *IEEE Transactions on Power Systems*, vol. 13, no. 2, pp. 543–551, 1998.

[13] A. Bose, "Smart transmission grid applications and their supporting infrastructure," *IEEE Transcations on Smart Grid*, vol. 1, pp. 11–19, 2010.

[14] H. Jiang, J. J. Zhang, D. W. Gao, Y. Zhang, and E. Muljadi, "Synchrophasor based auxiliary controller to enhance power system transient voltage stability in a high penetration renewable energy scenario," in *Power Electronics and Machines for Wind and Water Applications (PEMWA), 2014 IEEE Symposium*. IEEE, 2014, pp. 1–7.

[15] I. Smon, G. Verbic, and F. Gubina, "Local voltage-stability index using tellegen's theorem," *IEEE Transactions on Power Systems*, vol. 21, no. 3, pp. 1267–1275, 2006.